PAUL SCHERRER INSTITUT

Emilio Andrea Maugeri:: Function :: Paul Scherrer Institut

Targetry of Exotic Radionuclides at PSI

NUSPRASEN SHE-Workshop, GSI, Darmstadt

Paul Scherrer Institut (PSI) (*1988*)

Germany ↑ Aarau/Bern ↓ Zurich →

Paul Scherrer (1890–1969)

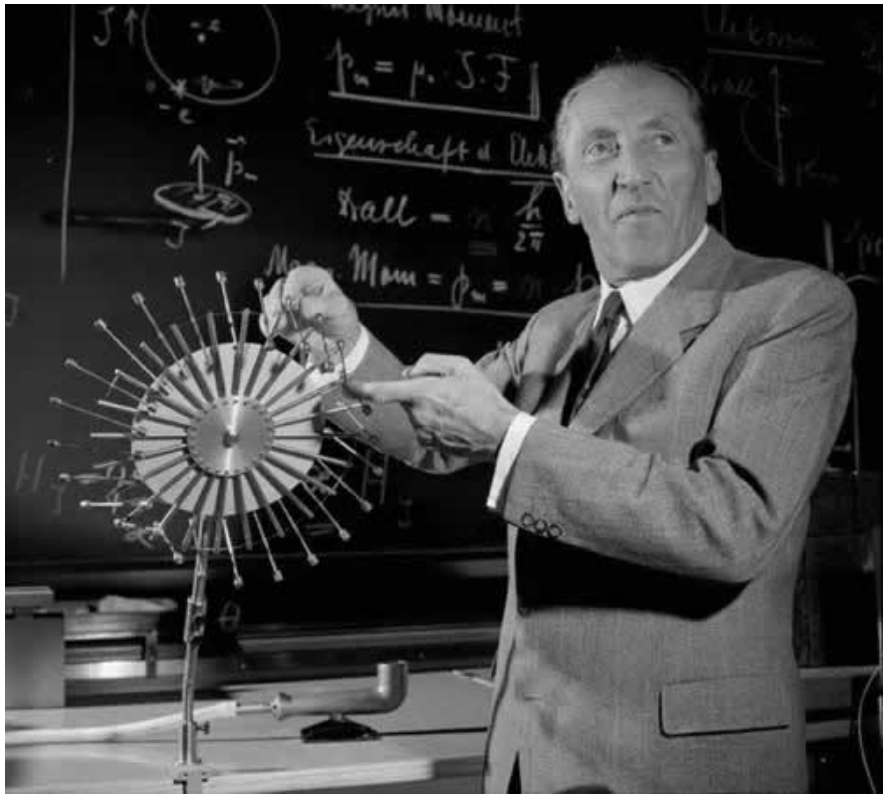

- Studied physics and mathematics at the Swiss Federal Institute of Technology (ETH) Zurich, in Koenigsberg and in Goettingen, Germany
- 1920: professor of experimental physics at ETH Zurich; 1927: Director of the Institute of Physics. Was famous for the clarity of his lectures
- Researched x-ray scattering on crystals, liquids and gases (Debye-Scherrer method).
- Later research work was in nuclear physics 1946: President of the Swiss Study Commission on Atomic Energy
- Involved in the foundation of CERN

PSI in a nutshell

Distribution to main research areas (first- and third-party funding)

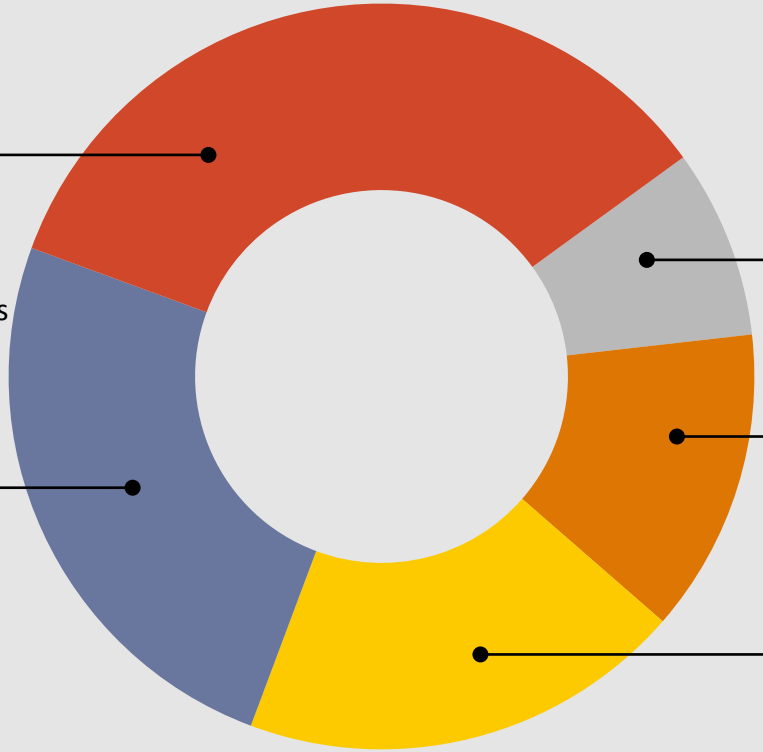

Materials Research
35%

- better materials for long-life batteries
- better materials for fuel cells
- new materials for data storage in technologies of the future

Life Sciences
25%

Particle Physics
8%

Nuclear Energy and Safety
13%

Energy and Environment
19%

PSI in a nutshell

← Basel Germany ↑ Aarau/Bern ↓ Zurich →

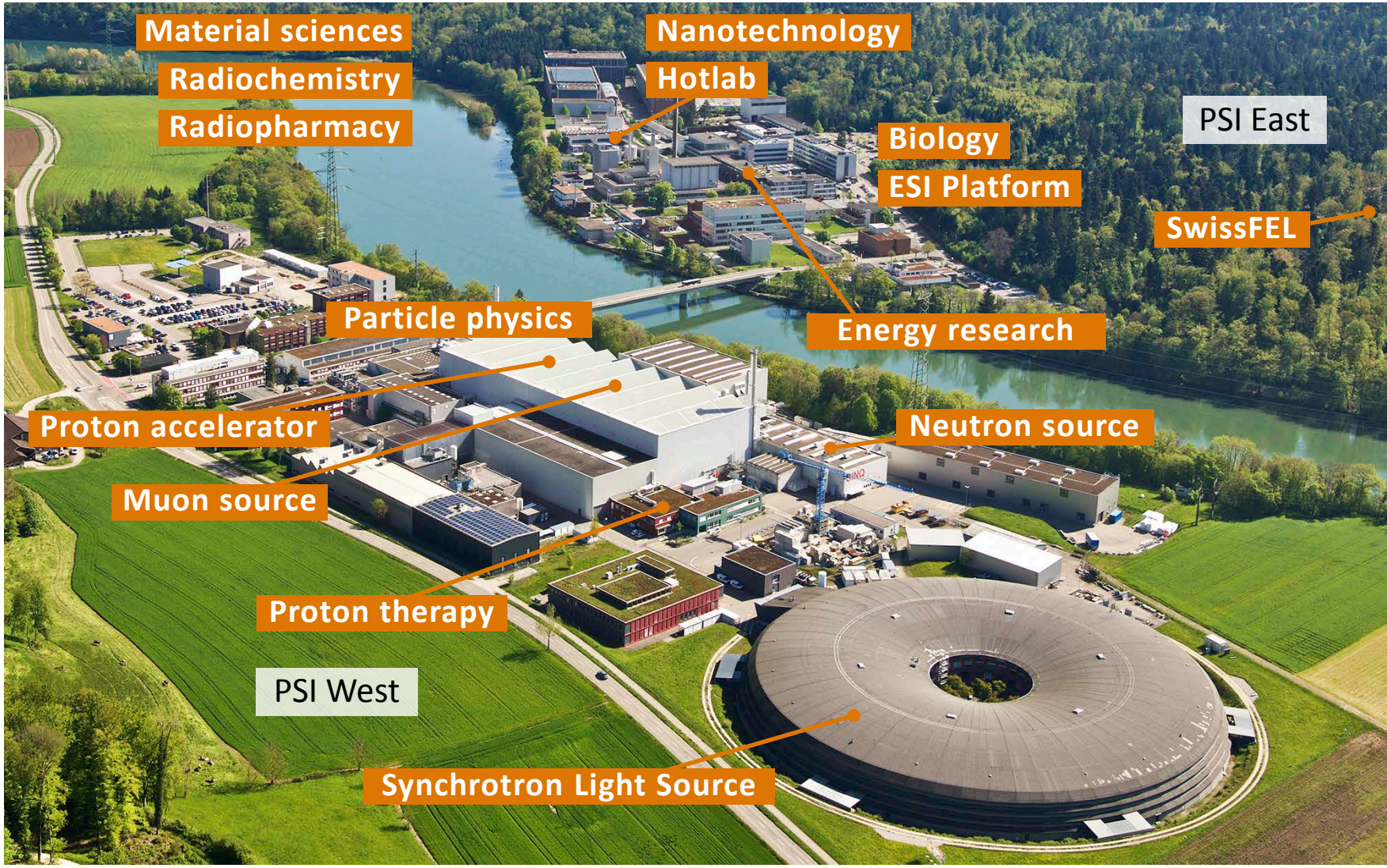

“Useful” components

Copper beam dump

- ^{44}Ti, ^{53}Mn, ^{26}Al, ^{60}Fe, ^{59}Ni, ^{32}Si, ^{60}Co

Proton of 590 MeV and a beam current of up to 2.4 mA.

Myon production station

- Operation 1-3 years
- Source for ^{10}Be

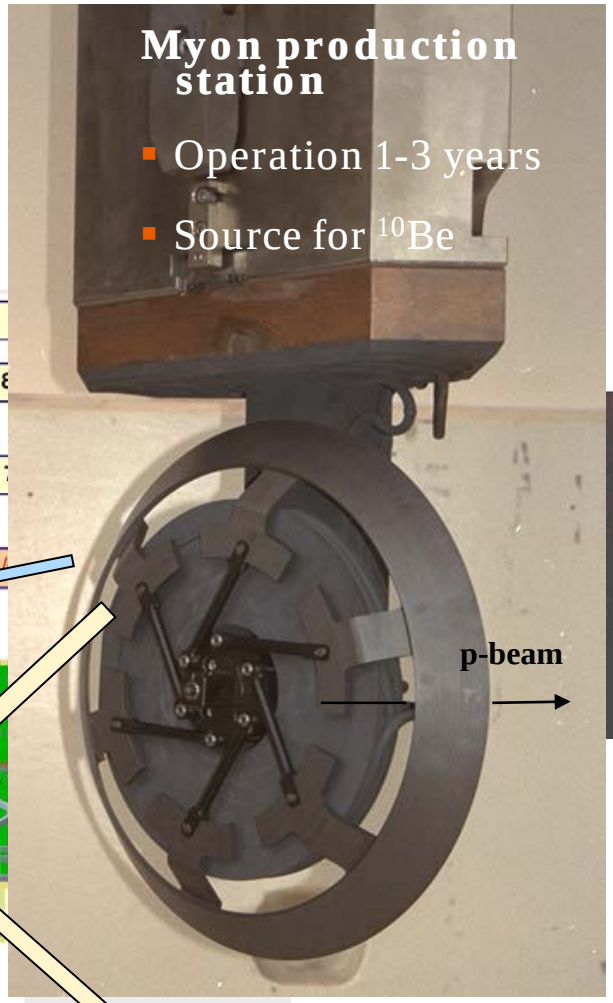

SINQ cooling water

^{7}Be, ^{22}Na, ^{88}Y

Special irradiations positions with 590 MeV protons

V for ^{44}Ti and ^{32}Si production

Bi for ^{205}Pb production

SINQ target

- ^{207}Bi, ^{172}Hf,
- ^{173}Lu, ^{194}Hg,
- ^{202}Pb, ^{125}Sb,
- ^{106}Ru, ^{44}Ti

“Useful” components

Copper beam dump

- ^{44}Ti, ^{53}Mn, ^{26}Al, ^{60}Fe, ^{59}Ni, ^{32}Si, ^{60}Co

^{44}Ti, ^{26}Al and ^{53}Mn for nuclear astrophysics: for describing galactic evolution and for understanding of the history of the universe.

Information on ^{44}Ti ($t_{1/2}$ = 59.1±0.3 y) nucleosynthesis in supernova. The production of the isotope ^{44}Ti is considered to be a distinctive signature of core-collapse SN, from stars more massive than 8–10 solar masses.

Myon production station

- Operation 1-3 years
- Source for ^{10}Be

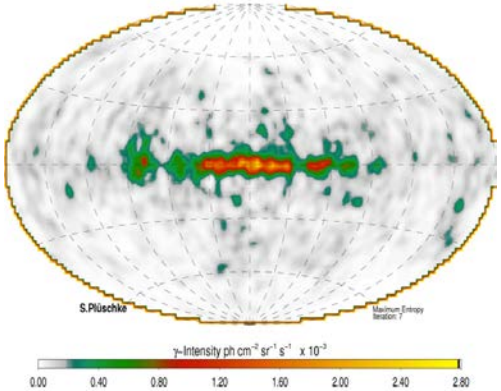

Galactic ^{26}Al distribution

[http://hera.ph1.uni-koeln.de/~heintzma/Integral/Artikel/Al26.htm]

Nuclide production facilities, Basic nuclear physics research , Nuclear astrophysic , AMS measurement, Environmental chemistry

SINQ Target Irradiation Program-STIP

^{44}Ti, ^{53}Mn, ^{26}Al

^{60}Fe is an important chronometer for periods of several Mill. y

^{32}Si is a new chronometer for nuclear dating

Special irradiations positions with 590 MeV protons

V for ^{44}Ti production

Bi for ^{205}Pb production

SINQ cooling water

^{7}Be, ^{22}Na, ^{88}Y

SINQ target

- ^{207}Bi, ^{172}Hf,
- ^{173}Lu, ^{194}Hg,
- ^{202}Pb, ^{125}Sb,
- ^{106}Ru, ^{44}Ti

Conclusions

- We can provide different "exotic" isotopes:
  - by their extraction from components of the proton accelerator at PSI, e.g. ^{26}Al, ^{59}Ni, ^{53}Mn, ^{60}Fe,

    ^{44}Ti, ^{10}Be, ^{7}Be ^{14}C, ^{207}Bi, ^{182}Hf ^{146}Sm, several Dy isotopes, ^{22}Na, ^{88}Y and many others….
  - or produce them in dedicated p- or n- high energy (up to 560 MeV) irradiation experiments, e.g.

    ^{44}Ti from V and ^{205}Pb from Bi.

- We can produce targets out of them, with different size, shape and activity, using different techniques, e.g. molecular plating and vaporization of different size droplets.

Targetry

- Material
- Method
- Target characterization

Starting material

- The target material must be as chemically and isotopically pure as reasonably possible. Impurities could, in fact, enhance the background during the cross section measurement.

Starting material

PHYSICAL REVIEW C **92**, 015806 (2015)

Thermal neutron capture cross section of the radioactive isotope ^{60}Fe

T. Heftrich,[1,*] M. Bichler,[2] R. Dressler,[3] K. Eberhardt,[4] A. Endres,[1] J. Glorius,[1,5] K. Göbel,[1] G. Hampel,[4] M. Heftrich,[1] F. Käppeler,[6] C. Lederer,[7] M. Mikorski,[1] R. Plag,[1] R. Reifarth,[1] C. Stieghorst,[4] S. Schmidt,[1] D. Schumann,[3] Z. Slavkovská,[1] K. Sonnabend,[1] A. Wallner,[8] M. Weigand,[1] N. Wiehl,[4] and S. Zauner[4]

[1]*Goethe Universität Frankfurt, Frankfurt, Germany*
[2]*Technische Universität Wien, Vienna, Austria*
[3]*Paul Scherrer Institut, Villigen, Switzerland*
[4]*Johannes Gutenberg-Universität Mainz, Mainz, Germany*
[5]*GSI Helmholtzzentrum für Schwerionenforschung, Darmstadt, Germany*
[6]*Karlsruhe Institute of Technology, Karlsruhe, Germany*
[7]*University of Edinburgh, Edinburgh, United Kingdom*
[8]*Australian National University, Canberra, Australia*

(Received 26 January 2015; published 23 July 2015)

Background: Fifty percent of the heavy element abundances are produced via slow neutron capture reactions in different stellar scenarios. The underlying nucleosynthesis models need the input of neutron capture cross sections.

Purpose: One of the fundamental signatures for active nucleosynthesis in our galaxy is the observation of long-lived radioactive isotopes, such as ^{60}Fe with a half-life of 2.60×10^6 yr. To reproduce this γ activity in the universe, the nucleosynthesis of ^{60}Fe has to be understood reliably.

Methods: An ^{60}Fe sample produced at the Paul Scherrer Institut (Villigen, Switzerland) was activated with thermal and epithermal neutrons at the research reactor at the Johannes Gutenberg-Universität Mainz (Mainz, Germany).

Results: The thermal neutron capture cross section has been measured for the first time to $\sigma_{\rm th} = 0.226\,(^{+0.044}_{-0.049})$ b. An upper limit of $\sigma_{\rm RI} < 0.50$ b could be determined for the resonance integral.

Conclusions: An extrapolation towards the astrophysically interesting energy regime between $kT = 10$ and 100 keV illustrates that the s-wave part of the direct capture component can be neglected.

DOI: 10.1103/PhysRevC.92.015806 PACS number(s): 25.40.Lw, 26.20.Kn, 27.50.+e, 28.20.Ka

Starting material

TABLE III. The number of Zr nuclei produced in the activations and the resulting neutron fluences without and with cadmium shielding.[a]

	Without Cd	With Cd
$N(^{95}\mathrm{Zr})$[b]	$1.517 \pm 0.005 \pm 0.018$	$0.510 \pm 0.006 \pm 0.008$
$N(^{97}\mathrm{Zr})$[b]	$1.171 \pm 0.001 \pm 0.018$	$1.067 \pm 0.001 \pm 0.016$
Φ_{th}[c]	$8.60 \pm 0.03 \pm 0.38$	$1.21 \pm 0.01 \pm 0.16$
Φ_{epi}[c]	$0.467 \pm 0.002 \pm 0.014$	$0.458 \pm 0.005 \pm 0.014$

[a]Uncertainties are statistical and systematic, respectively.
[b]In units of 10^9.
[c]In units of 10^{14} cm^{-2}.

B. Thermal (n,γ) cross section of ^{60}Fe

The γ spectrum measured after the activation of the ^{60}Fe sample without cadmium shielding (Fig. 6) clearly exhibits the γ transitions of ^{61}Fe at 297.9, 1027, and 1205 keV. However, only the last two were used in the analysis because of the poor signal-to-background ratio of the 298-keV line. The systematic uncertainty is calculated by the error of the efficiency, the I_γ, the half-lives, and the neutron fluences (see Tables I, III, and IV). In the corresponding spectrum measured after the activation with cadmium shielding, the ^{61}Fe lines are completely missing as illustrated in Fig. 7 for the 1027-keV line as an example. In this case, only an upper limit can be determined for the resonance integral. The numbers of produced ^{61}Fe nuclei are listed in Table IV.

TABLE IV. The number of ^{61}Fe nuclei (in units of 10^5) produced in the activations.

γ-ray energy	$N(^{61}\mathrm{Fe})$[a]	
(keV)	Without Cd	With Cd
1027	$1.54 \pm 0.19 \pm 0.18$	<0.179
1205	$1.48 \pm 0.20 \pm 0.16$	<0.206
Weighted average	$1.51 \pm 0.14 \pm 0.24$	<0.179[b]

[a]Uncertainties are statistical and systematic, respectively.
[b]Adopted upper limit for further discussion.

The number ratio of ^{61}Fe and ^{60}Fe after the activation without cadmium is

$$N(^{61}\mathrm{Fe})/N(^{60}\mathrm{Fe}) = \Phi_{th}\sigma_{th} + \Phi_{epi}\sigma_{RI}. \quad (12)$$

The thermal cross section

$$\sigma_{th}(^{60}\mathrm{Fe}) = \frac{N(^{61}\mathrm{Fe})}{N(^{60}\mathrm{Fe})}\frac{1}{\Phi_{th}} - \sigma_{RI}\frac{\Phi_{epi}}{\Phi_{th}} \quad (13)$$

is determined by the number of sample atoms $N(^{60}\mathrm{Fe})$ (Sec. II B), the neutron fluences Φ_{th} and Φ_{epi} from the Zr monitor measurements (Table III), and the number of ^{61}Fe nuclei produced during the activations $N(^{61}\mathrm{Fe})$ (Table IV).

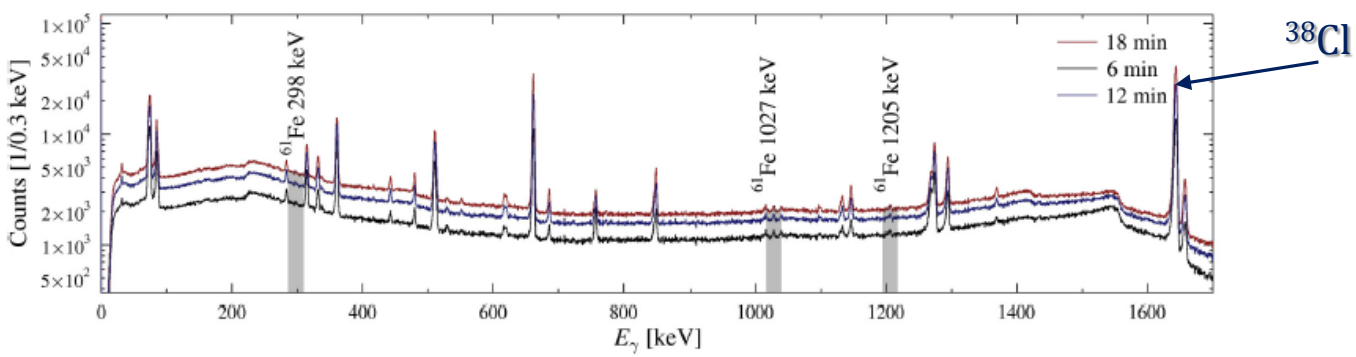

Starting material

Nuclear Instruments and Methods in Physics Research A 613 (2010) 347–350

Contents lists available at ScienceDirect

Nuclear Instruments and Methods in Physics Research A

journal homepage: www.elsevier.com/locate/nima

Preparation of a ^{60}Fe target for nuclear astrophysics experiments

D. Schumann [a,*], J. Neuhausen [a], I. Dillmann [b], C. Domingo Pardo [b], F. Käppeler [b], J. Marganiec [b], F. Voss [b], S. Walter [b], M. Heil [c], R. Reifarth [c], J. Goerres [d], E. Uberseder [d], M. Wiescher [d], M. Pignatari [d,e]

[a] *Laboratory for Environmental and Radiochemistry, Paul Scherrer Institute Villigen, 5232 Villigen PSI, Switzerland*
[b] *Forschungszentrum Karlsruhe, Institut für Kernphysik, Postfach 3640, D-76021 Karlsruhe, Germany*
[c] *GSI Helmholtzzentrum für Schwerionenforschung GmbH, Planckstrasse 1, 64291 Darmstadt, Germany*
[d] *University of Notre Dame, Department of Physics, Notre Dame, IN 46556, USA*
[e] *Keele University, Keele, Staffordshire ST5 5BG, UK*

ARTICLE INFO

Available online 9 October 2009

Keywords:
Nuclear astrophysics
Radio-chemical separation
Neutron capture cross-section

ABSTRACT

An ^{60}Fe target for studying the ^{60}Fe(n, γ)^{61}Fe cross-section at stellar energies was prepared using radio-chemical separation techniques. In total, 7.8×10^{15} ^{60}Fe atoms (777 ng) were separated from a copper beam dump for the 590 MeV proton beam of the high intensity accelerator at PSI. The final target was prepared by evaporating the iron-containing aqueous solution onto a graphite backing. With this sample the keV neutron capture cross-section of ^{60}Fe has been measured at FZ Karlsruhe.

The work is part of the ERAWAST-initiative (Exotic Radionuclides from Accelerator WAste for Science and Technology) which is aimed at extracting rare valuable radionuclides from accelerator waste by chemical means.

Starting material

3. Special requirements for the ^{60}Fe separation

The chemical separation methods and the treatment of the sample are determined by several constraints concerning the planned experiments and made the preparation a very challenging issue:

Since ^{60}Fe with a half-life of $\sim 1.5 \times 10^6$ yr has no measurable γ-lines and only low-energetic β⁻-radiation, the exact number of ^{60}Fe atoms inside the target has to be determined via the ingrowth of the decay product ^{60} Co, according to ^{60}Fe (1.5×10^6 yr) $\xrightarrow{\beta^-}$ ^{60m}Co (10.5 min) $\xrightarrow{\beta^-,\gamma}$ ^{60}Co (5.3 yr) $\xrightarrow{\beta^-,\gamma}$ ^{60}Ni (stable). Therefore, the initial contamination of the target with ^{60}Co had to be as low as possible.

Fig. 2 shows an overview of the nuclear reactions and corresponding nuclear decay data relevant for the measurement of the neutron capture cross-section. The reaction product ^{61}Fe decays with a half-life of 6 min to ^{61}Co by emitting γ-rays of 298, 1027, 1205 keV, respectively. However, the γ-lines of ^{60}Co (1173, 1332 keV) produce a Compton background, which interferes with the γ-signals of the ^{61}Fe activity. Additionally, ^{44}Ti and its decay product ^{44}Sc emit γ-lines at 67, 75, and 1157 keV, which interfere with the radiation of the ^{61}Co ($t_{1/2}$ = 1.65 h, 67 keV) as well as with those from ^{61}Fe. Therefore, extremely high separation factors of several orders of magnitude for these contaminants were mandatory for the feasibility of the experiment.

Neutron captures on ^{58}Fe (natural abundance 0.28%) produce an additional background due to the γ-lines of ^{59}Fe (1009, 1292 keV), which also interfere with the γ-lines of interest. Therefore, considerable amounts of stable carrier had to be avoided, although the chemical yield of the separation may be dramatically reduced if radionuclides are used without carrier.

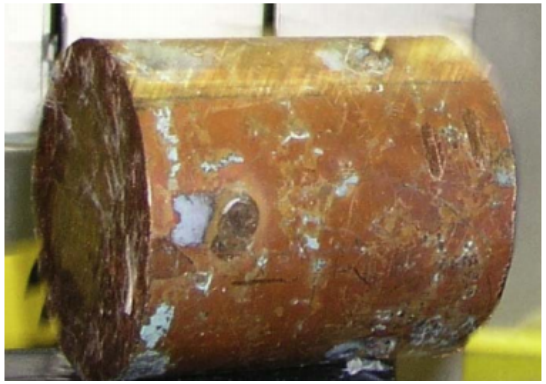

4. Chemical separation and results

In principle, several chemical methods can be applied for an efficient iron separation, i.e. precipitation of the hydroxide or liquid–liquid extraction as well as ion exchange of the chloro-complex. Since precipitation procedures require a minimal amount of stable carrier (corresponding to the solubility of the compound) or at least the addition of a non-isotopic carrier, the latter two methods are preferable in cases where carrier-free radionuclides have to be handled. For the present separation problem, liquid–liquid extraction was the method of choice. In principle, the preparation followed the procedure already briefly described in Ref. [9], slightly adapted to the required special conditions.

After dissolution of the copper in 7 M HNO_3, the solution was evaporated to dryness and re-dissolved in 7 M HCl. Five milligrams of stable cobalt carrier in form of Co^{2+} were added in order to achieve a mostly complete Co separation. Under these conditions, Fe^{3+} forms a water-soluble anionic chloro-complex, which can be extracted into organic media, in our case methylisobutylketone. All other elements of interest, e.g. ^{44}Ti, ^{44}Sc, ^{60}Co and the copper bulk, have very low distribution coefficients and remain predominantly in aqueous solution. The iron can then be re-extracted with diluted HCl. The procedure has to be repeated several times to obtain the required separation factor. The last separation has to be carried out immediately before starting the experiment, because the increase of ^{60}Co due to the decay of ^{60}Fe increases the background rate. After this final purification, the diluted HCl solution (0.1 M) was successively evaporated to dryness onto a graphite backing by slight heating. The dry graphite backing containing the ^{60}Fe was fixed on a thin Kapton foil stretched over an Al target holder and then covered with another Kapton foil. The final ^{60}Fe target is shown in Fig. 3.

The γ-spectrum taken immediately after the last chemical separation is plotted in Fig. 4. Apart from small contaminations with ^{60}Co and ^{44}Ti of 0.3 Bq each, which corresponds to decontamination factors of 3×10^8 and 5×10^6, respectively, the spectrum exhibits a high counting rate in the low-energy range due to internal bremsstrahlung from the electron capture decay of ^{55}Fe, which represents an additional complication for the measurement of the neutron capture cross-section of ^{60}Fe. The four background lines – as marked in the expanded spectrum as BG – were assigned to ^{228}Ac, ^{214}Bi, and ^{208}Tl, which are members of the natural decay chains.

The characteristics of the final target are summarized in Table 1. Special attention has to be paid to the number of ^{60}Fe atoms, which were determined via the ingrowth of the daughter

Targetry

Separation/ Purification

- Material
- Method
- Target characterization

Separation of ^{44}Ti

Investigation of the ^{44}Ti(α,p)^{47}V reaction in inverse kinematics at CERN ISOLDE

STIP sample

dissolution in 8 M HCl + conc. HNO_3. Heating for 30 min at 60 ºC. Filtering to remove undissolved particles. Washing with 8M HCl

Fe, Cr, Ni, Mo, Mn, Co, Al, Ti, V, W

extraction into di-ethyl-ether

organic phase
anionic chloride complexes:
$FeCl_4^-$ $MoO_2Cl_3^-$

aqueous phase
Cr, Ni, Mn, Co, Al, Ti, traces of Fe and Mo

precipitation with NH_3

Filtrate
stable ammonia complexes
CrO_4^{2-} $[Ni(NH_3)_6]^{2+}$
MoO_4^{2+} $[Co(NH_3)_6]^{2+}$

precipitate
$Al(OH)_3$ $Fe(OH)_3$ $Ti(OH)_4$ $Cr(OH)_3$ $Mn(OH)_2$

dissolution in 1 M HCl
precipitation with H_2O_2 + NaOH

filtrate
$[Al(OH)_4]^-$ CrO_4^{2-}

precipitate
$Fe(OH)_3$ $Ti(OH)_4$ MnO_2

dissolution in 7 M HCl
extraction with di-ethyl-ether

final organic phase
Fe

final aqueous phase
Ti, Mn

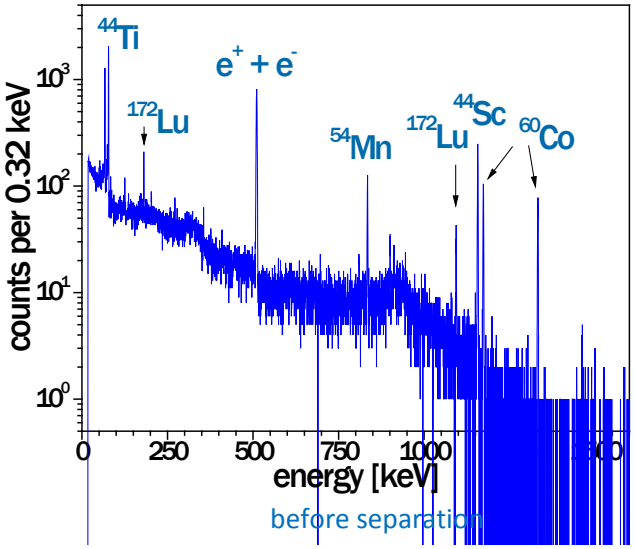

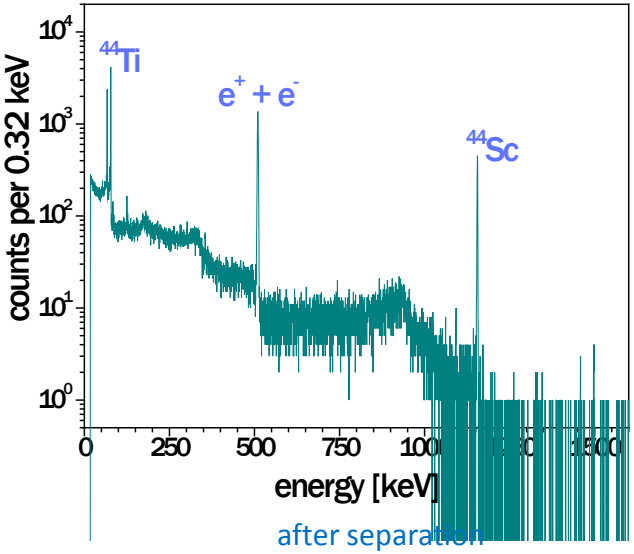

Totally available amount: several hunded MBq
Separated activity: 100 MBq (2.7 10^{17} atoms, 20 µg)

Separation of Ti and Mn was performed using ion-exchange chromatography.

R. Dressler *et al.* J. Phys. G: Nucl. Part. Phys. 39 (2012) 105201

Targetry

- Material
  - Separation/ Purification
  - Characterization (ICP-MS, ICP-OS, α- β- γ-spect. LSC)
- Method
- Target characterization

Targetry

- Material
- Method
- Target characterization

Target preparation methods

Molecular plating

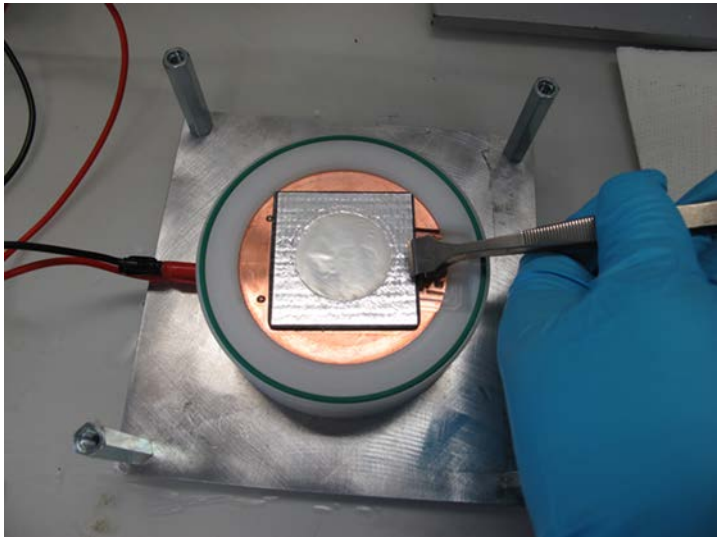

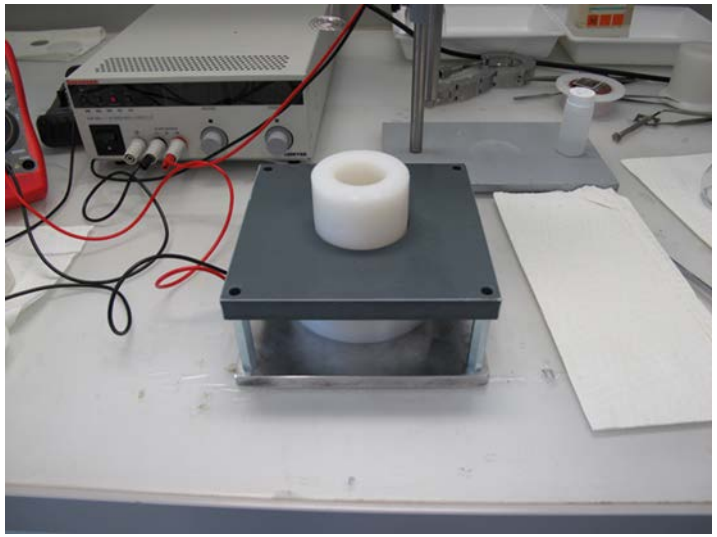

Deposition of Droplets

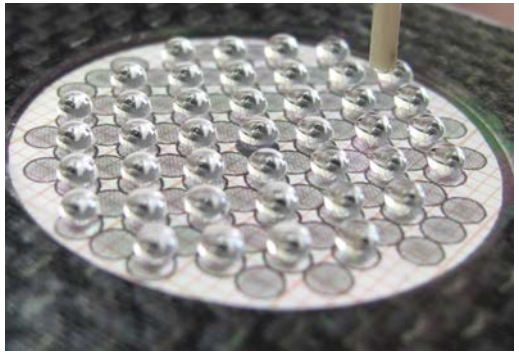

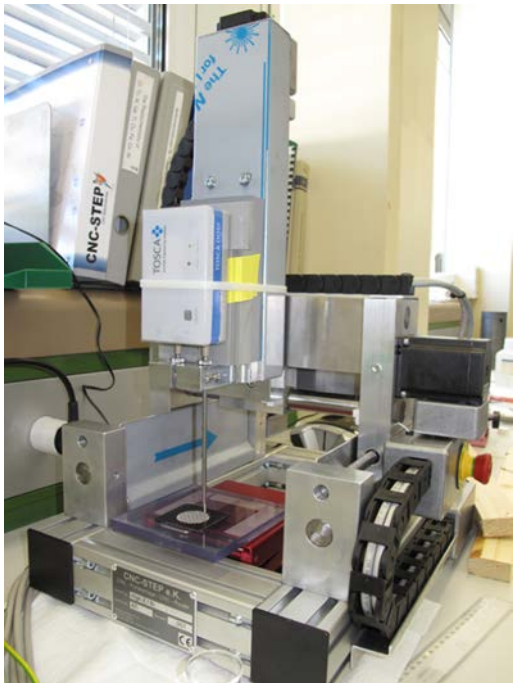

Target preparation methods

Physical vapor deposition

Manual hydraulic press

Off-line mass separation at ISOLDE

^{7}Be target:

- ≈ 100 ng of ^{7}Be (≈ 1.3 GBq)
- Chemically pure (^{7}Li free)
- **Isotopically pure ($^{9\text{-}10}$Be free)**
- **On a backing**
- **Thin, uniform and homogeneous layer**

ISOLDE General Purpose Separator (GPS)

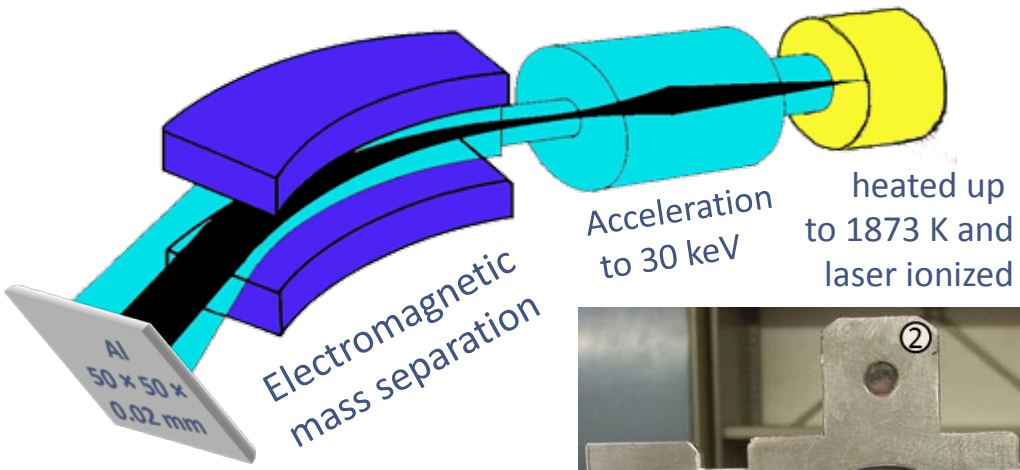

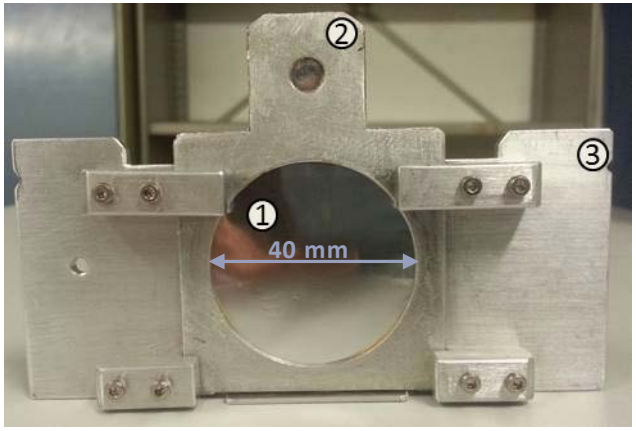

Target assembly: (1) aluminium backings; (2) aluminium frame, (3) target holder.

(1) Al backings: 50 × 50 × 0.018 mm

(2) Al Frame: 50 × 50 × 1 mm with a 40 mm diameter central hole

(3) Target holder

7.2×10^{15} ions, ≈ 1GBq, were estimated to be implanted over 10 h

Targetry

- Material
- Method
- Target characterization

Target characterization: Activity measurement

The measurement was performed by means of a coaxial HPGe-detector. The target was placed at 389 cm from the detector in order to keep the total impulse rate on the measurement chain on a reasonable range.

Result: (1.03 ± 0.02) GBq. 6.8×10^{15} ions (against the 7.2×10^{15} foreseen)

Target Characterization

- The incident particles should have the same probability of interaction with the target nuclei and the energy loss of all the detected particles should be similar. This implies that the deposited target material must be homogeneous and have uniform thickness.

Target Characterization: measurement of thickness

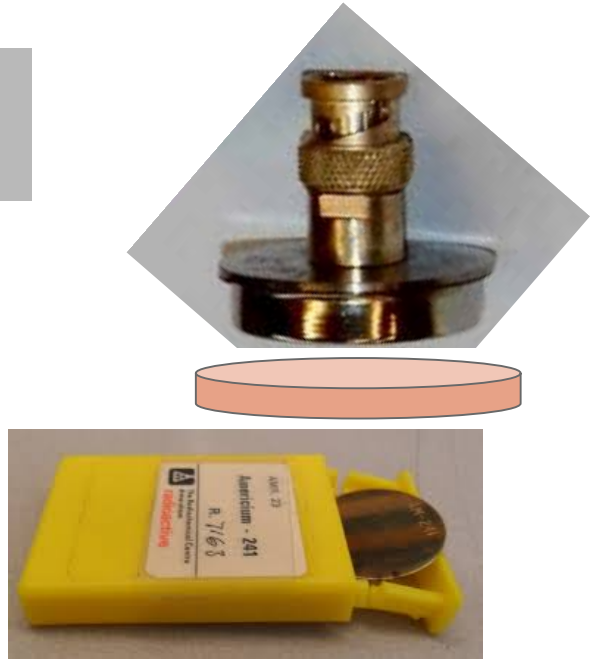

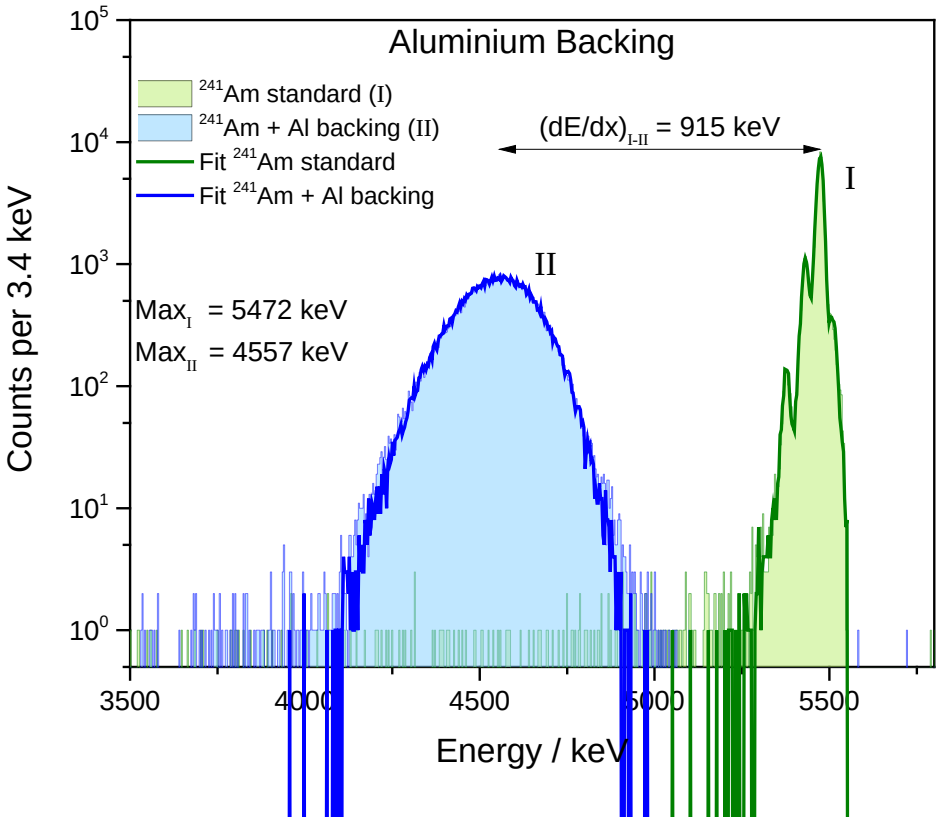

The fit was obtained with an Al-thickness value of (5.25 ± 0.07) µm and a fluctuation of (0.50 ± 0.02) µm. The value of fluctuation indicates a variation of the thickness of about 10%.

Target Characterization: measurement of thickness

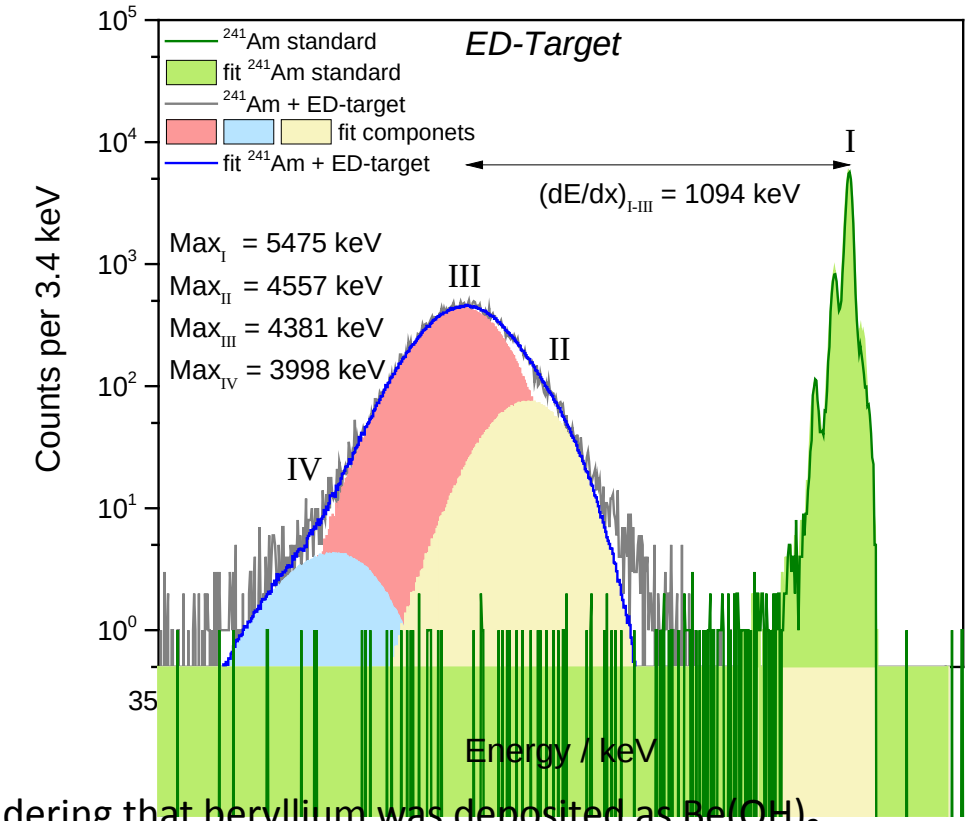

The ED-Target spectrum was simulated considering that beryllium was deposited as $Be(OH)_2$.

The main peak, III, at 4381 keV, about 84% of the distribution, was attributed to the energy loss resulting from the combined effect of the Al backing and the average deposition layer with a thickness of (1.04 ± 0.40) µm (energy degradation of 176 keV).

Target characterization:Distribution map

Radiographic imaging method:

GE Typhoon™ FLA 7000 Imaging Plate Reader with spatial resolution down to 25 µm was used in combination with reusable Fujifilm imaging plates.

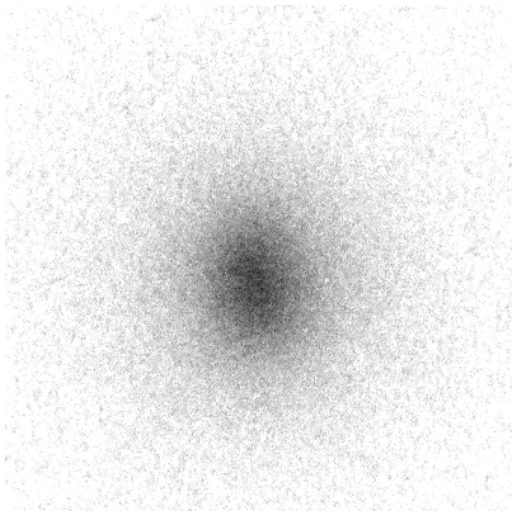

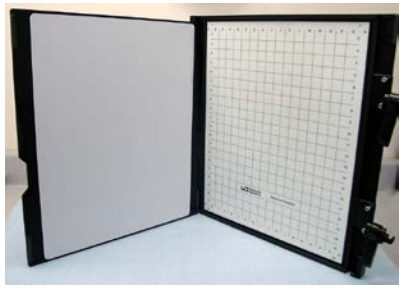

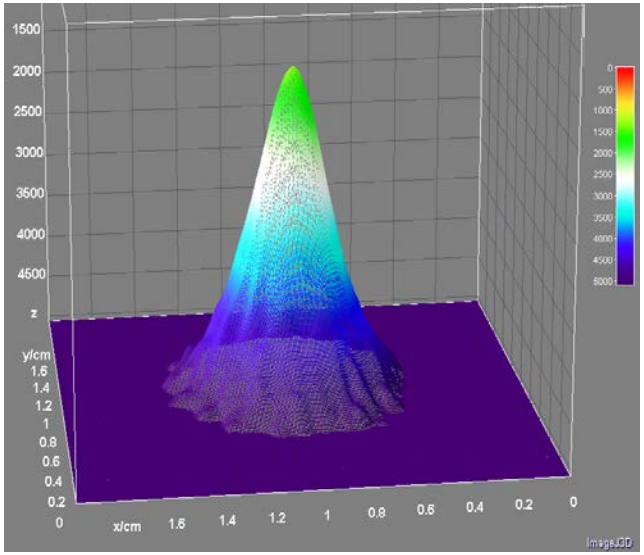

^{7}Be distribution: Radiographic imaging

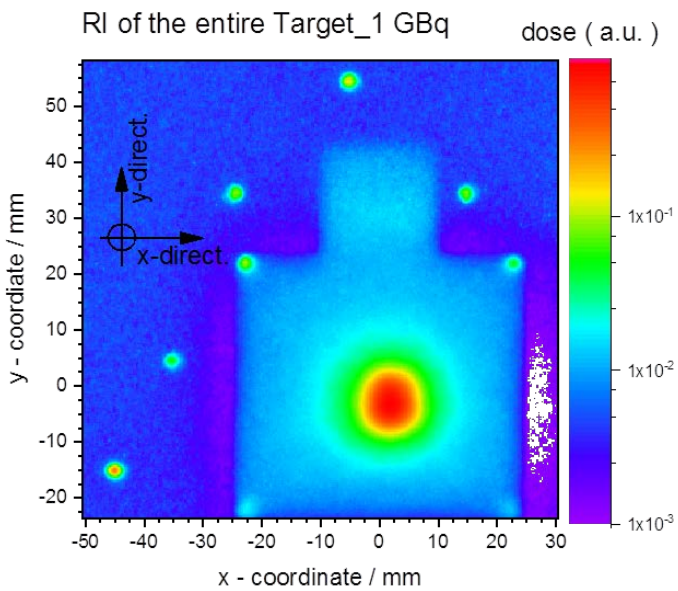

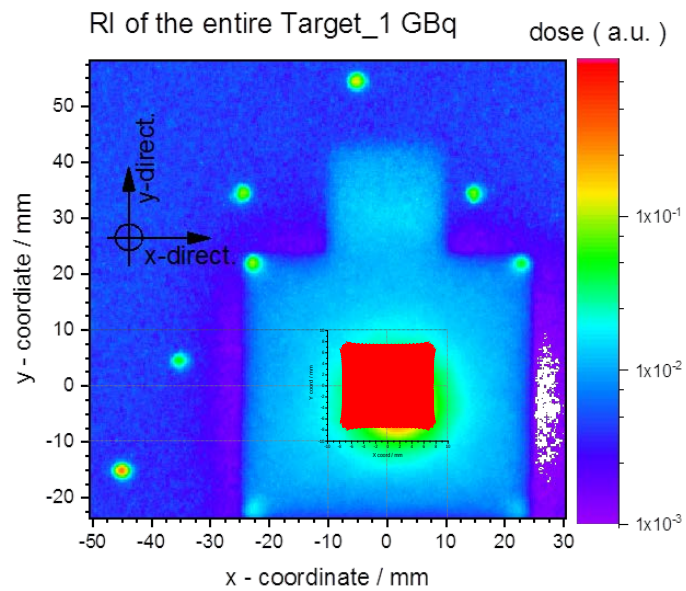

The implanted area has a planar cross section of an ellipse and is shifted with respect to the geometrical centre of the target.

Width parameters and implanted positions

Target Name	x-centre [mm]	x-width [mm]	y-centre [mm]	y-width [mm]	rotation [°]
RI of Target_1GBq	1.699 ± 0.183	2.064 ± 0.011	-5.200 ± 0.112	2.440 ± 0.012	0.13

^{7}Be distribution: Radiographic imaging

RI 2D graphs superimposed to the n_TOF neutron beam profile

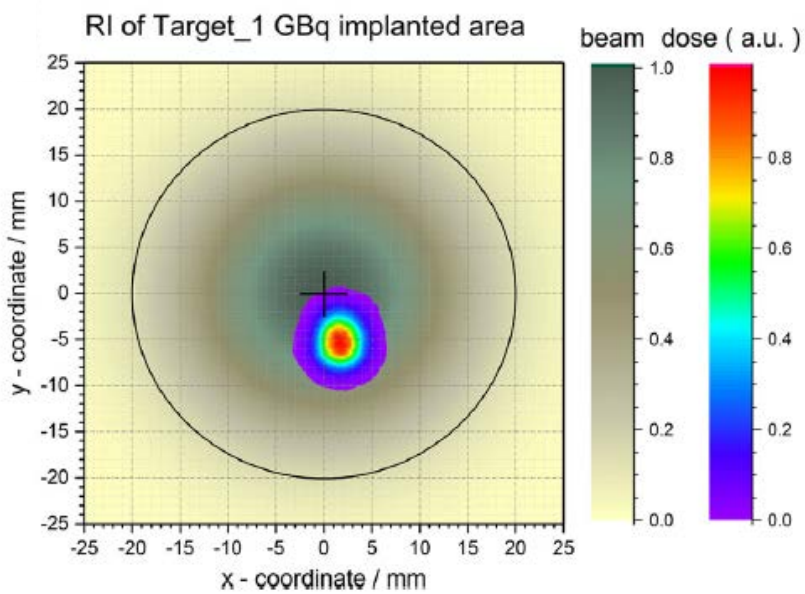

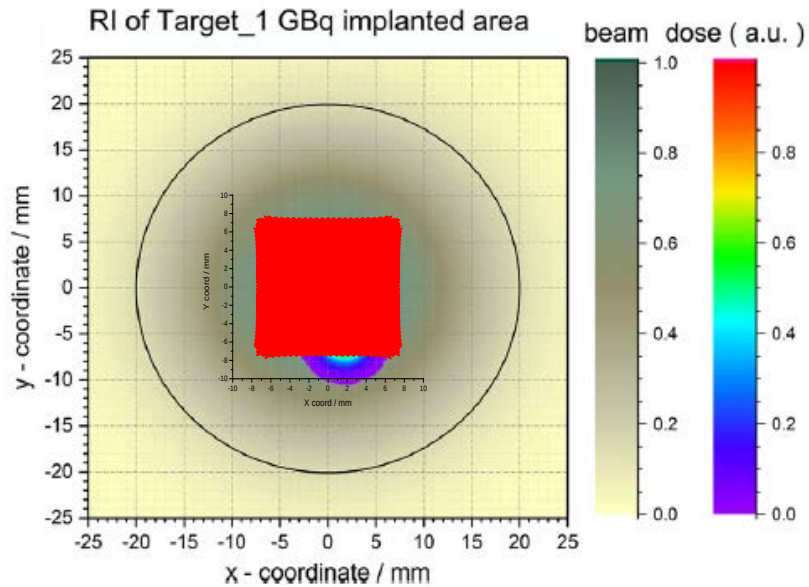

The centre of the beam profile was overlapped to the geometrical centre of the target

The implanted area of Target was exposed only to about 85% to 75% of the neutron beam intensity

The People of LRC